

Investigating social alignment via mirroring in a system of interacting language models

Harvey McGuinness*[†]
Johns Hopkins University

Tianyu Wang*
Johns Hopkins University

Carey E. Priebe
Johns Hopkins University

Hayden Helm
Helivan Research

Abstract

Alignment is a social phenomenon wherein individuals share a common goal or perspective. Mirroring, or mimicking the behaviors and opinions of another individual, is one mechanism by which individuals can become aligned. Large scale investigations of the effect of mirroring on alignment have been limited due to the scalability of traditional experimental designs in sociology. In this paper, we introduce a simple computational framework that enables studying the effect of mirroring behavior on alignment in multi-agent systems. We simulate systems of interacting large language models in this framework and characterize overall system behavior and alignment with quantitative measures of agent dynamics. We find that system behavior is strongly influenced by the range of communication of each agent and that these effects are exacerbated by increased rates of mirroring. We discuss the observed simulated system behavior in the context of known human social dynamics.

A key phenomenon underlying the formation of human groups is social alignment (Ransom et al., 2019). This phenomenon, through which individuals adopt the behaviors of the individuals they interact with, has been shown to support the creation of social relationships through the promotion of positive commonality (Burton-Jones et al., 2020). In short, like attracts like, and it is through social alignment that individuals behave more alike one another in order to foster cohesive relationships.

One of the most direct mechanisms to achieve social alignment is social mirroring (Hasson and Frith, 2016). This occurs primarily subconsciously, as individuals will mimic (or mirror) the facial

expressions, posture, mannerisms, and other behaviors of those with whom they interact (Tunçgenç et al., 2022). However, social mirroring is not limited to physical mimicry, as it can also include a more complete degree of copying wherein individuals parrot speech patterns, opinions, and perspectives of those they are mirroring to appear maximally agreeable (Byrne, 2005).

While social mirroring has been studied extensively in small group conditions – primarily with respect to one-on-one interacting pairs (Gallotti et al., 2017) – little research has been done exploring its system-level consequences, primarily due to the infeasibility of large-scale experiments. Instead, system-level social science research has been predominantly concerned with the broad consequences of social alignment in group performance once a group has already been established (Ledgerwood and Wang, 2018), rather than the decentralized processes from which those groups can emerge.

Previous theoretical work exploring foundational human social behaviors has been conducted through either purely mathematical means such as the long-tested voter model of population dynamics (Redner, 2019) or via overly simple computational frameworks (Yang et al., 2021). While these approaches can produce excellent insights into the general social dynamics of a population, recent advances in machine learning techniques have enabled explorations of classic economic, psycholinguistic, and social psychology experiments. For example, the recent cohort of Large Language Models (LLMs), such as OpenAI’s GPT4, are able to replicate the Ultimatum Game, Garden Path Sentences, and Milgram Shock Experiment (Aher et al., 2023).

Although recent LLMs are able to generate human-like outputs (Webb et al., 2023; Helm et al., 2023) and replicate classic experiments without explicit training (see, e.g., (Webb et al., 2023)), human-like behavior is not sufficient to model individuals in a social system. Indeed, it is necessary to

* denotes equal contribution.

[†] corresponding author: hmcguin1@jhu.edu.

have generative variation across agents that effectively mimics cognitive differences across people. Prior research has shown that retrieval augmented generation (“RAG”) improves the performance of LLMs by allowing them to retrieve documents that are relevant to a query from a domain-specific or knowledge-intensive database (Gao et al., 2024). For social experiments, a RAG database can be considered the knowledge base or memory of an individual in the social system: the LLM will generate responses based on the combination of its pre-training data and the RAG database, just as people express their thoughts based on a history of previous experiences and the current environmental context. Previous work studying LLM agents, such as (Park et al., 2023), have shown that pairing a single LLM with a RAG database-per-individual can effectively promote generation diversity.

In this paper we present a computational framework to study the macroscopic effects of social alignment through social mirroring. Our framework is parameterized by important characteristics of interactions in a social system, such as the likelihood of an individual being mirrored and the range of individuals with whom someone may interact. The framework is general to collections of agents that have the capacity to exchange information, though our analysis focuses on systems of interacting LLMs due to their ability to exchange information in natural language at a human-like capacity.

We first introduce our experiment of interacting LLMs to study the effect of mirroring on social alignment in detail. We then present and discuss the results before interpreting them from the perspective of comparable social science case studies.

1 Experimental Design

We let A_1, \dots, A_n be n agents. Each agent is Meta’s LLaMA-2-7B-Chat (Touvron et al., 2023) equipped with a different external database. As mentioned above, the external databases are a proxy for different knowledge bases and memories of individuals in a community. In our experiment, each database contains sentences about flowers. These sentences are randomly sampled from a collection of sentences originally generated by prompting ChatGPT with “Provide many sentences about various kinds of flowers.”.

We simplify the set of possible sequences of social interactions by only allowing agent interactions

at discrete time steps $t = 1, \dots, T$. The experimental protocol is composed of a measurement step and an interaction step:

- **(Measurement Step)** At each time t , we ask each agent to describe the prettiest flower in a single sentence based on its database. We denote the answer as $B_i^{(t)}$ ($i = 1, \dots, n$; $t = 0, \dots, T$). The answers will be used to measure agent alignment.

We use the open source embedding model `openai-embed-v1.5` (Nussbaum et al., 2024) to quantitatively measure differences amongst the $B_i^{(t)}$. The embedding model maps each sentence $B_i^{(t)}$ to a vector $X_i^{(t)} \in \mathbb{R}^{768}$. A smaller distance between $X_i^{(t)}$ and $X_j^{(t')}$ means that $B_i^{(t)}$ and $B_j^{(t')}$ are more semantically similar and, hence, more aligned. We capture the pairwise alignment with $D^{(t)}$:

$$(D^{(t)})_{ij} := \|X_i^{(t)} - X_j^{(t)}\|_2,$$

where $\|\cdot\|_2$ denotes the vector l_2 -norm.

We note that sentences can be different in many aspects. For example, the sentences “The prettiest flower is rose because roses come in a vast range of colors” and “The prettiest flower is lily because lilies come in a vast range of colors” are different because they are about two types of flowers. The first sentence is also different from “The prettiest flower is rose because its layered petals spiral in a graceful design” because they describe different properties of roses.

- **(Interaction Step)** At each time $t > 0$, we update each agent’s database based on their interaction with another agent. The agents in which agent A_i can communicate with is determined by its k -nearest neighbors (says $D^{(t)}$). In particular, A_i will interact with exactly one of its nearest neighbors. Given that A_j is in A_i ’s nearest neighbors, the probability that A_i interacts with A_j is $1/k$. The type of interaction that A_i has with A_j is determined as follows:
 - With probability p (constant for all agents), agent A_j mirrors A_i . Functionally, this means A_i “updates” itself with its own answer $B_i^{(t)}$. This update

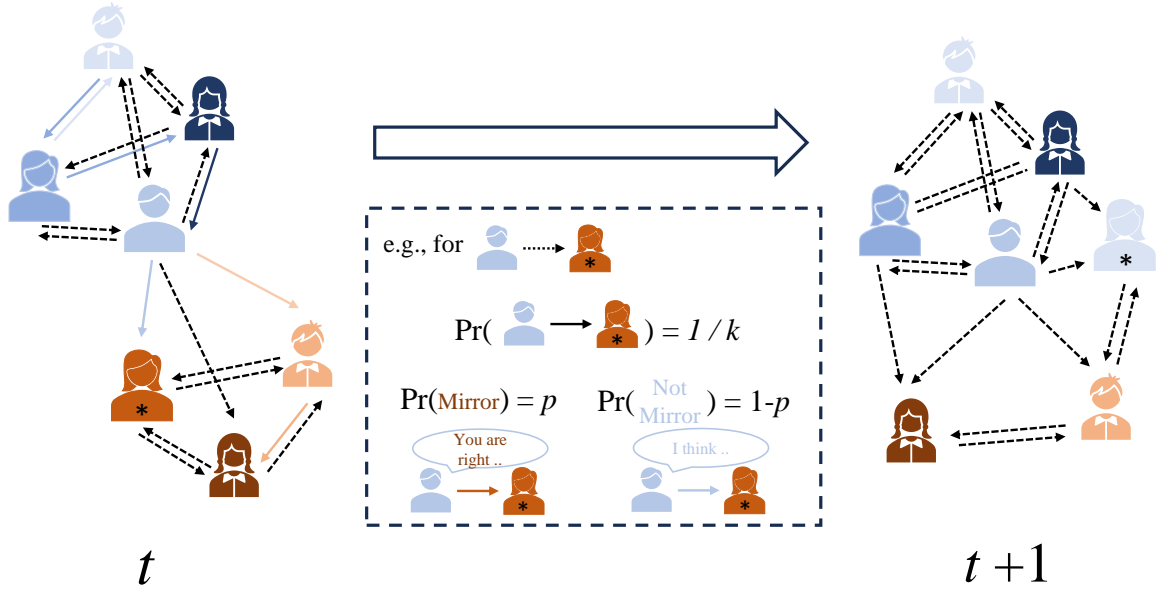


Figure 1: Illustration of simulated system dynamics with $n = 7$ agents with a communication range of $k = 3$. Dashed arrows connect agents in the communication range of the receiving agent. Solid arrows connect the agent that interacted with the receiving agent. Arrow color represents the type of interaction – if it is the color of the receiving agent then communicating agent is mirroring, otherwise they are not mirroring. Mirroring occurs with probability p for each interaction. The opinion of an agent and the agents in its range of communication may change at time $t + 1$ based off its interaction at time t . For example, the blue arrow from the light-blue male to the orange female at t affects the opinion of the orange female at $t + 1$ – she becomes light blue and the agents in her communication range change. See Section 1 for further details.

function serves to model agent A_j 's social alignment to A_i (Hasson and Frith, 2016).

- With probability $1 - p$, A_j does not mirror A_i and, instead, responds with $B_j^{(t)}$. A_i is then updated with $B_j^{(t)}$. This update function is a model of basic information exchange wherein individuals communicate without copying behavior (or, do not align) before responding.

An illustration of system dynamics is provided in Figure 1. Note that the evolution of the described system depends on the probability of interacting with a mirroring agent (p), and the number of nearest neighbors an agent is able to interact with (k ; sometimes referred to as the agents' "range of communication"). We measure system evolution by clustering the agents' responses based on the which flower it describes as the prettiest – we are agnostic to differences in the reason for choosing the flower. In particular, we assign each flower a Flower ID and use it to designate an agent's cluster (or "silo") membership. Silo membership can change as a function of t .

We let $c_i^{(t)}$ denote the silo in which A_i is a mem-

ber of at time t and $\omega_c^{(t)}$ denote the number of agents in silo c at time t . We define the stability of the system at time t , $S^{(t)}$, to be the proportion of agents where $c_i^{(t)} = c_i^{(t-1)}$:

$$S^{(t)} := \frac{1}{n} \sum_{i=1}^n \mathbb{1}\{c_i^{(t)} = c_i^{(t-1)}\}.$$

We similarly let $E^{(t)}$ be the entropy of the system at time t (Manning et al., 2008),

$$E^{(t)} := - \sum_c \frac{\omega_c^{(t)}}{n} \log_2 \frac{\omega_c^{(t)}}{n}.$$

We analyze the evolution of systems using $S^{(t)}$ and $E^{(t)}$ as a function of p and k below.

2 Results

2.1 Observed silo patterns

Before discussing the effects of p and k on the evolution of the system, we first highlight three patterns of silos that we observed from our experiment: I) "Stable silos", II) "Unstable silos", and III) "Decaying silos". We characterize Patterns I-III via the number of silos at t , $S^{(t)}$, and $E^{(t)}$:

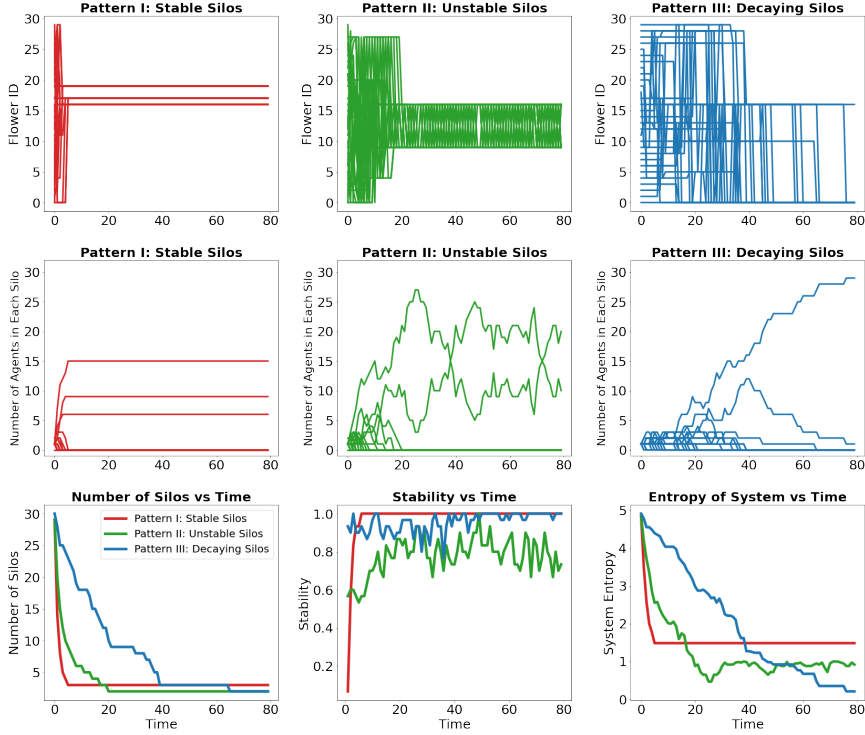


Figure 2: Three patterns of silos: Stable (Pattern I), Unstable (Pattern II), and Decaying (Pattern III). System classification occurs at $T = 80$. **Top.** Example systems for the three of the observed types of patterns. Each line represents an agent. **Middle.** The dynamics of the number of agents in each silo for each of the example systems in the top row. Each line represents a silo. **Bottom.** The metrics used to classify a system for each of the example systems in the top row. Systems with stable silos have multiple non-empty silos with unchanging members; systems with unstable silos have multiple non-empty silos with interchanging members; systems with decaying silos have recently experienced the observed minimum entropy.

- I. A system has stable silos if, after some $t^* > 0$, the number of silos is constant, $E^{(t)}$ is constant, and $S^{(t)} = 1$. A system with stable silos is in a steady state.
- II. A system has unstable silos if, after some $t^* > 0$, the number of silos is constant, $E^{(t)}$ is approximately constant, and $S^{(t)} < 1$. A system with unstable silos is in a steady state.
- III. A system has decaying silos if $T - \min(\operatorname{argmin}_t E^{(t)}) < m$ for a suitably chosen m . That is, the system is decaying if the first time the system entropy achieves its minimum is within m steps from the end of the system's evolution. In our experiment $T = 80$ and we chose $m = T/10 = 8$. A system with decaying silos is not in a steady state.

We also observed systems that converge into a single silo. We refer to these systems as “One silo” systems and note that they are in a steady state. Systems observed to have Pattern III will eventually decay into a system with stable silos, unstable silos,

or a single silo. Further, while different subsystems within a system may exhibit different (un)stability or decay, we classify the systems using the number of silos, entropy, and stability of the entire system.

We show an example of Patterns I-III in the top row of Figure 2. Each line corresponds to an agent's silo evolution up to $T = 80$. The leftmost figure shows a system exhibiting Pattern I, where the Flower ID for each agent stabilizes and remains the same. Conversely, the center figure shows a Pattern II system where some agents in a Pattern II system oscillate between at least two silos for $t > 20$. The rightmost figure shows an example of a decaying system: one of the silos is slowly absorbing the others.

The second row of figures show how the number of agents in a silo evolves over time for each of the example systems in the first row. Each line in a given figure corresponds to a silo. In the system with stable silos, the number of agents stabilizes quickly. In the system with unstable silos, the number of members in two of the silos oscillate, as agents “jump” from one silo to the other and back.

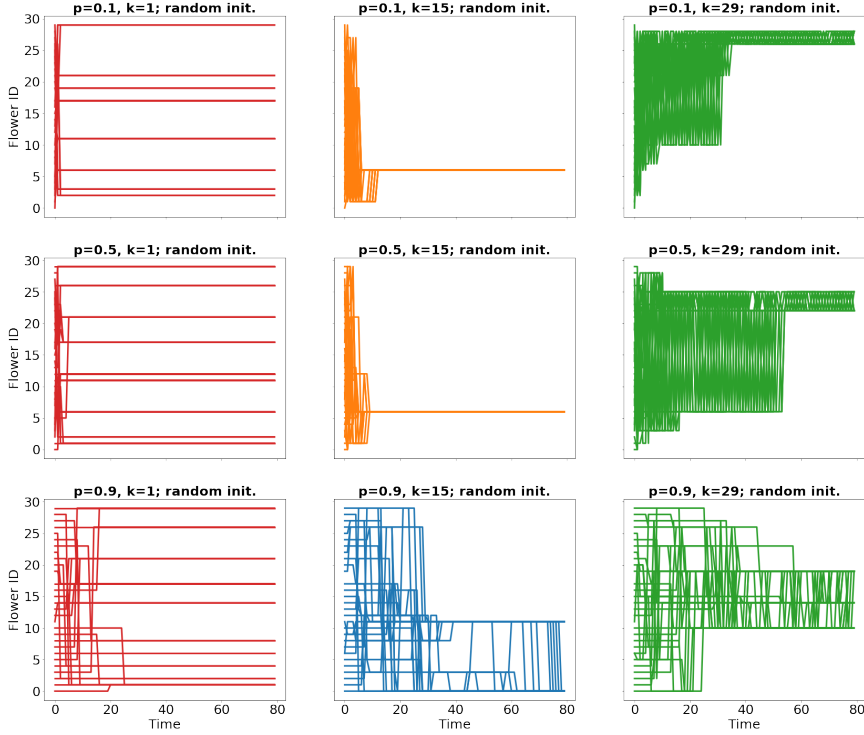


Figure 3: Example systems of $n = 30$ with different agent behaviors. Graph color (red/blue/green/orange) indicates the pattern of stable/decaying/unstable/one silo(s) at $T = 80$. Small range of communication for each agent (k) appears to prohibit global alignment. Large likelihood of mirroring (p) delays global alignment. We investigate these relationships further in Figures 4 and 5.

Neither of the oscillating silos appear primed for substantial decay or growth in the long-run – a hallmark characteristic of the group dynamics in a system with unstable silos. Lastly, the system with decaying silos has a silo that is nearly always growing while the other silos do not attract more members after $t \approx 40$.

The last row of figures shows the pattern-defining metrics associated with each highlighted system: number of silos (left), stability (center), and entropy of system (right).

2.2 The effects of p and k

Figure 3 shows the evolution of systems of $n = 30$ agents for nine different settings of agent behaviors (i.e., p and k). Overall, when the agents’ range of communication is small we observe stable silos; when $k/n \approx 0.5$ and p is small we observe one silo; and when $k \rightarrow n$ we observe unstable or decaying silos. Further, when the likelihood of interacting with a mirroring agent is small, systems converge quickly; when p is large, systems stay in transient states for longer.

We explore the relationship between system type and number of silos at $T = 80$ in more detail in Figures 4 and 5, where each dot corresponds to

an entire system. In particular, for each setting of agent behavior we consider 8 different random agent initializations and label each system according to the observed system behavior up to $T = 80$. We include a line representing the average number of observed silos at $T = 80$ to help emphasize the effects of p and k .

Figure 4 shows the relationship of silo count and k for various p . As observed in Figure 3, when k is small the systems typically contain stable silos. For $k/n \approx 0.5$ systems typically contain a single silo. For $k/n > 0.5$, systems are more likely to contain unstable silos or decaying silos as k increases, though this effect is dependent on p .

Our results suggest that the range of communication of the agents acts as a moderating pressure on the number of supportable silos: when the range is partially restrictive the agents are able to form a consensus, when the range is too restrictive or too loose the system experiences population polarization or multi-silo instability, respectively. As a consequence, fractured systems will remain fractured in settings where agents have a restricted communication range and multiple unstable silos are likely to persist in settings where agents have a

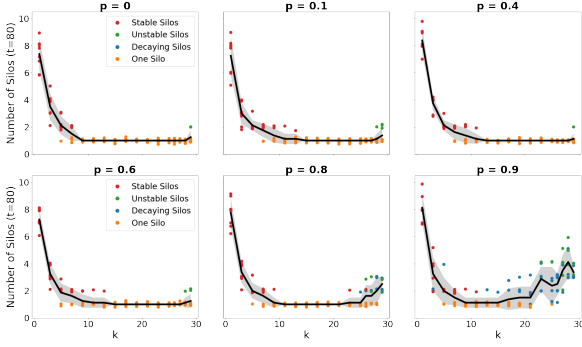


Figure 4: Number of Silos vs. k (the range of communication) for several values of p (the likelihood of an agent interacting with a mirroring agent). For each setting of agent behavior we include the number of silos observed at $T = 80$ for 8 random agent initializations. Dot color corresponds to system type at $T = 80$. The black line is the average number of silos with the shaded area representing ± 3 standard errors. Up to a point, increasing k encourages global alignment. When k is large the system is more likely to contain multiple silos at $T = 80$.

nearly unbounded range of communication.

In Figure 5, we investigate the relationship of silo count and p for various k . For small k , p does not appear to have a large impact on the number of silos observed at $T = 80$. For k/n close to one, however, p has a clear effect on the number of silos. As p increases the expected number of silos increases. Further, these silos are typically unstable or decaying.

The splintering of high- p , high- k populations is primarily due to the increase in time which a high- p population requires to converge. In particular, when the majority of interactions are instances of a mirroring interaction, there is little opportunity for actual information to be shared. Thus, agents are more likely to remain isolated in their own perspective bubble for a longer amount of time – with only the off-chance that basic interactions serving to collapse perspective bubbles into multi-agent silos – resulting in few instances where a consensus across the entire population is reached by $T = 80$. We note that when $p = 1$, the number of silos is equal to the number of flower IDs present in the initial conditions, as the opportunity for an informative interaction has been completely replaced by mirroring interactions.

3 Discussion

In Section 2.2.1 we introduced a system classification based on the observed silo behavior in a

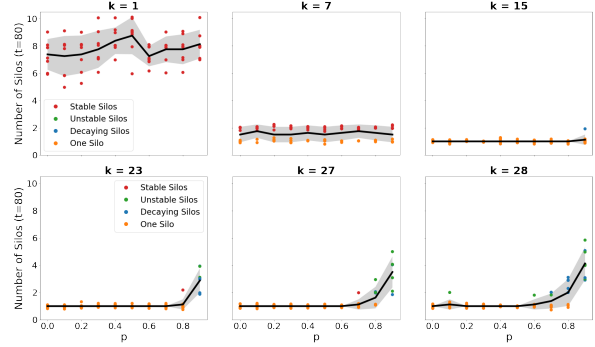


Figure 5: Number of Silos vs. p (the likelihood of an agent interacting with a mirroring agent) for several values of k (the range of communication). For each setting of agent behavior we include the number of silos observed at $T = 80$ for 8 random agent initializations. Dot color corresponds to system type at $T = 80$. The black line is the average number of silos with the shaded area representing ± 3 standard errors. Increasing p decreases the likelihood of global consensus across all k .

system of interacting agents. In Section 2.2.2 we discussed the effects of the range of agent communication and of the likelihood of interacting with a mirroring agent on the number and type of silos observed at $T = 80$.

Our results show that increasing the rates of social mirroring can have substantial impact on the group dynamics of a system of interacting agents. The effect is particularly pronounced in settings where the range of communication for each agent is suitably large. For settings where agents have more restricted communication, high rates of social mirroring have a minimal impact on the degree and type of group formation. We interpret these results as due to a perspective-filtering effect inherent to systems with local communication. Indeed, local communication settings are essentially high-mirroring settings since agents only interact with others similar to them. When p is large we observe multiple groups at $T = 80$, though the type of groups that arise depends on k .

The observed effect of p and k on the dynamics of the system has notable parallels with known behaviors of observed in social groups. For example, research investigating the role of information overexposure in polarization has shown that populations exposed to increasing amounts of information tend towards being more polarized (Xu et al., 2021; Levy and Razin, 2020). We observe similar behaviors in our simulated systems, particularly as the trend of group count decreasing as k increases

reverses near the global communication limit, resulting in multiple unstable and/or decaying groups – closely matching the observed behaviors in populations inundated with vast amounts of information (Xu et al., 2021; Levy and Razin, 2020).

Similarly, (Carlson and Knoester, 2011) and (Cinelli et al., 2021) discuss potential causes of the formation of physical and online echo chambers. Essentially, members in family-sized groups reinforce the opinions of fellow members. For physical groups, opinion is fortified based on pre-existing geographical proximity (Carlson and Knoester, 2011). For online echo chambers, members self-select based on their pre-existing opinions and thus are only ever subjected already-aligned people (Cinelli et al., 2021). Different parameter settings of our simulated system allow us to understand the effect of these behaviors when applied to every agent in the system – small k models opinions reinforced by geographical communication constrains and large p models opinions reinforced after self-selecting for interactions with agents with similar opinions. As seen in Figures 4 & 5 these settings lead to many small stable groups that are unable to achieve population consensus due to their isolation from alternative perspectives.

Finally, recent studies explore the links between social media usage and value mirroring (Modgil et al., 2021) and detail the increasing rates of mirroring via self-censorship (Gibson and Sutherland, 2023). These studies suggest that group-membership prediction is an increasingly difficult task as people are unwilling to publicly break from perceived policy and social norms – potentially providing a reason why polling accuracy has not increased despite the availability of more data on the electorate (Jennings and Wlezien, 2018). Indeed, the results from our simulated systems suggest that high rates of social mirroring could cause poor estimation of support for a particular candidate or piece of legislation since systems with large p are more likely to have multiple unstable or decaying silos at $T = 80$.

Our research demonstrates that social mirroring serves as a modifier for the pre-existing trend dictated by the range of communication in a population. Overall, the range of interaction serves as a predictive variable with respect to the state of silos in a population – whether they are stable, unstable, or decaying, as well as the silo count. The frequency of social mirroring, however, distorts this base trend by exaggerating it as mirroring in-

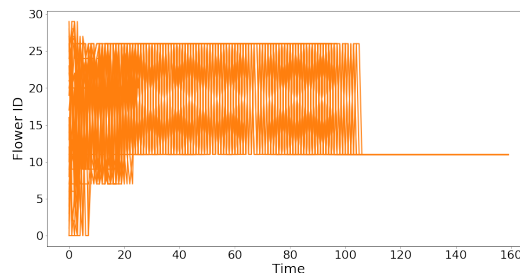


Figure 6: Example system with $p = 0.2$, $k = 29$, $T = 160$. The system has unstable silos at $T = 80$ and a single silo for $T > 105$ – indicating that longitudinal analysis may provide additional insights into system behavior.

creases in frequency. A population experiencing global communication will likely have multiple unstable groups regardless of p , but the magnitude of silo splintering and the severity of instability will be shaped significantly by p .

4 Future Work

Our framework enables simple and interpretable investigation of the effect of the range of agent communication and the likelihood of interacting with a mirroring agent on group dynamics and social alignment. With that said, there are many interesting directions for follow-on work.

For example, we limited our analysis to systems with $n = 30$ agents. While 30 agents is large enough for relatively complicated group dynamics to emerge, simulating larger systems will allow us to draw parallels to the dynamics observed in human systems more easily. Similarly, we focused on system classification at $T = 80$. The classification of a system will depend on the choice of T , as seen in Figure 6 where we observe unstable silos at $t = 80$ and a single silo for $t > 110$. Extending our work to longitudinal analysis (i.e., across various T) of the systems may be necessary to fully understand group dynamics.

Further, our framework can be used to study the effect other social phenomena – such as miscommunication – on alignment by adjusting the update mechanism. Recall that in our analysis the database for each agent is updated to perfectly reflect its most recent interaction. We could introduce variably sized perturbations of the response from the most recent interaction to model different levels of agent miscommunication. Such analysis would provide insight into how repeated exposure to information may impact alignment.

We could similarly increase the complexity of the agent’s databases and retrieval mechanisms to better model human behavior. For example, the generative agents studied in (Park et al., 2023) store, process, and manage a history of complicated interactions with their environment. While there are benefits to the simple agents that we study, increasing the complexity of the agents while maintaining the simple interaction mechanisms studied herein may improve the generalizability of our simulations to sociological settings. We note that increasing the complexity of the agents will require using general black-box techniques (Duderstadt et al., 2024; Helm et al., 2024b; Acharyya et al., 2024; Helm et al., 2024a) to study agent, group, and system dynamics.

Lastly, we note that the behavior of the systems that we studied can be approximated with a system of interacting Gaussian Mixture Models (GMMs). On one hand, replacing the current agents with GMMs may decrease the generalizability of the results to human social systems. On the other hand, it could make the simulations more computationally efficient and more mathematically tractable. The cost effectiveness of a system of interacting GMMs, even relative to the simple agents studied herein, could enable the analyses of systems with an otherwise impossible number of agents and time steps. The tractability of the GMM systems could enable theoretical analysis of the group dynamics and limiting behavior in terms of $E^{(t)}$ and $S^{(t)}$.

Acknowledgments

We would like to thank Avanti Athreya, Brandon Duderstadt, Henry Farrell, Vince Lyzinski, and Youngser Park for their helpful feedback and discussions throughout the development of this manuscript.

References

Aranyak Acharyya, Michael W. Trosset, Carey E. Priebe, and Hayden S. Helm. 2024. [Consistent estimation of generative model representations in the data kernel perspective space](#). *Preprint*, arXiv:2409.17308.

Gati V Aher, Rosa I. Arriaga, and Adam Tauman Kalai. 2023. Using large language models to simulate multiple humans and replicate human subject studies. In *Proceedings of the 40th International Conference on Machine Learning*, volume 202 of *Proceedings of Machine Learning Research*, pages 337–371. PMLR.

Andrew Burton-Jones, Alicia Gilchrist, Peter Green, and Michael Draheim. 2020. [Improving social alignment during digital transformation](#).

Richard Byrne. 2005. Social cognition: Imitation, imitation, imitation. *Current Biology*.

Daniel Carlson and Chris Knoester. 2011. [Family structure and the intergenerational transmission of gender ideology](#). *Journal of Family Issues - J FAM ISS*, 32:709–734.

Matteo Cinelli, Gianmarco De Francisci Morales, Alessandro Galeazzi, Walter Quattrociocchi, and Michele Starnini. 2021. [The echo chamber effect on social media](#). *Proceedings of the National Academy of Sciences*, 118(9):e2023301118.

Brandon Duderstadt, Hayden S. Helm, and Carey E. Priebe. 2024. [Comparing foundation models using data kernels](#). *Preprint*, arXiv:2305.05126.

Mattia Gallotti, Merle Fairhurst, and Chris Frith. 2017. [Alignment in social interactions](#). *Consciousness and Cognition*, 48:253–261.

Yunfan Gao, Yun Xiong, Xinyu Gao, Kangxiang Jia, Jinliu Pan, Yuxi Bi, Yi Dai, Jiawei Sun, Meng Wang, and Haofen Wang. 2024. [Retrieval-augmented generation for large language models: A survey](#). *Preprint*, arXiv:2312.10997.

James L Gibson and Joseph L Sutherland. 2023. [Keeping your mouth shut: Spiraling self-censorship in the united states](#). *Political Science Quarterly*, 138(3):361–376.

Uri Hasson and Chris D Frith. 2016. [Mirroring and beyond: Coupled dynamics as a generalized framework for modelling social interactions](#).

Hayden Helm, Aranyak Acharyya, Brandon Duderstadt, Youngser Park, and Carey E. Priebe. 2024a. [Embedding-based statistical inference on generative models](#). *Preprint*, arXiv:2410.01106.

Hayden Helm, Brandon Duderstadt, Youngser Park, and Carey Priebe. 2024b. [Tracking the perspectives of interacting language models](#). In *Proceedings of the 2024 Conference on Empirical Methods in Natural Language Processing*, pages 1508–1519, Miami, Florida, USA. Association for Computational Linguistics.

Hayden Helm, Carey E. Priebe, and Weiwei Yang. 2023. [A statistical turing test for generative models](#). *Preprint*, arXiv:2309.08913.

Will Jennings and Christopher Wlezien. 2018. Election polling errors across time and space. *Nature Human Behaviour*, 2(4):276–283.

Alison Ledgerwood and Y Wang. 2018. Achieving local and global shared realities: distance guides alignment to specific or general social influences. *Current Opinion in Psychology*.

- Gilat Levy and Ronny Razin. 2020. [Social media and political polarisation](#).
- Christopher D. Manning, Prabhakar Raghavan, and Hinrich Schütze. 2008. *Introduction to Information Retrieval*. Cambridge University Press.
- Sachin Modgil, Rohit Kumar Singh, Shivam Gupta, and Denis Dennehy. 2021. [A confirmation bias view on social media induced polarisation during covid-19](#).
- Zach Nussbaum, John X. Morris, Brandon Duderstadt, and Andriy Mulyar. 2024. [Nomic embed: Training a reproducible long context text embedder](#). *Preprint*, arXiv:2402.01613.
- Joon Sung Park, Joseph O’Brien, Carrie Jun Cai, Meredith Ringel Morris, Percy Liang, and Michael S Bernstein. 2023. Generative agents: Interactive simulacra of human behavior. In *Proceedings of the 36th annual acm symposium on user interface software and technology*, pages 1–22.
- Tailer G. Ransom, Rick Dale, Roger J. Kreuz, and Deborah Tollefsen. 2019. How do different types of alignment affect perceived entity status? *Journal of Psycholinguistic Research*.
- Sidney Redner. 2019. [Reality-inspired voter models: A mini-review](#). *Comptes Rendus Physique*, 20(4):275–292.
- Hugo Touvron, Louis Martin, Kevin Stone, Peter Albert, Amjad Almahairi, Yasmine Babaei, Nikolay Bashlykov, Soumya Batra, Prajjwal Bhargava, Shruti Bhosale, et al. 2023. Llama 2: Open foundation and fine-tuned chat models. *arXiv preprint arXiv:2307.09288*.
- Bahar Tunçgenç, Martha Newson, Justin Sulik, Yi Zhao, Guillaume Dezeccache, Ophelia Deroy, and Marwa El Zein. 2022. Social alignment matters: Following pandemic guidelines is associated with better wellbeing. *BioMed Central*.
- Taylor Webb, Keith J. Holyoak, and Hongjing Lu. 2023. [Emergent analogical reasoning in large language models](#). *Preprint*, arXiv:2212.09196.
- Chao Xu, Jinyang Li, Dachun Sun, Ruijie Wang, Tarek Abdelzaher, Jesse Graham, and Boleslaw Szymanski. 2021. [On polarization dynamics in the age of information overload](#).
- Vicky Chuqiao Yang, Mirta Galesic, Harvey McGinness, and Ani Harutyunyan. 2021. [Dynamical system model predicts when social learners impair collective performance](#). *Proceedings of the National Academy of Sciences*, 118(35):e2106292118.